

THE THINNEST COLD H I CLOUDS IN THE DIFFUSE INTERSTELLAR MEDIUM?

SNEŽANA STANIMIROVIĆ AND CARL HEILES

Radio Astronomy Lab, University of California, Berkeley, 601 Campbell Hall, Berkeley, CA 94720;
 sstanimi@astro.berkeley.edu, heiles@astro.berkeley.edu

Received 2005 April 15; accepted 2005 June 3

ABSTRACT

We confirm and discuss recently discovered cold H I clouds with column densities among the lowest ever detected. The column densities of the cold neutral medium (CNM) toward 3C 286 and 3C 287 are $\sim 10^{18} \text{ cm}^{-2}$, below an observational lower limit and also below tiny-scale atomic clouds detected by VLBI and time-variable profiles against pulsars. These column densities are close to the minimum imposed by thermal evaporation. The ratios of the CNM to total H I toward 3C 286 and 3C 287 are $\sim 4\%$ and $\lesssim 2\%$, respectively. We discuss the CNM fraction and the CNM clouds in relation to several theoretical models.

Subject headings: ISM: clouds — ISM: structure — radio lines: ISM

1. INTRODUCTION

The cold neutral medium (CNM) is easily studied with the 21 cm line absorption because the H I opacity is $\propto N(\text{H I})/T$, where $N(\text{H I})$ is the column density and T is the temperature. The CNM has been an important subfield for the interstellar medium (ISM) in general and radio astronomy in particular. Theoretically, the CNM is understood as being one of two thermal equilibrium states of the neutral medium (Field et al. 1969; McKee & Ostriker 1977; Wolfire et al. 2003). McKee & Ostriker (1977) summarized the expected properties for the CNM clouds: a constant density of 42 cm^{-3} , a temperature of 80 K, a cloud size between 0.4 and 10 pc (with a mean value of 1.6 pc), and an H I column density ranging between 6.5×10^{19} and $173 \times 10^{19} \text{ cm}^{-2}$, with a mean value of $27 \times 10^{19} \text{ cm}^{-2}$.

Although thermal properties of the CNM are very well understood theoretically and observationally, its other aspects remain mysterious and not well studied, primarily because of a paucity of observational knowledge. This observational paucity includes such very basics as cloud shapes (morphology) and the column density distribution; accompanying it is the theoretical paucity involving the production mechanism of the CNM, the dynamic equilibrium between the CNM and its environment (specifically condensation, evaporation, and turbulent mixing), and the timescales for formation and destruction.

Two important recent observational works are stimulating further work on this topic. One is the Millennium Survey of 21 cm line absorption, of which the latest paper (Heiles & Troland 2005, hereafter HT05) provides statistical distributions of the fundamental parameters: column density, temperature, turbulence, and magnetic field. The second is the detection of reliable, very weak H I absorption lines toward three high-latitude sources by Braun & Kanekar (2005a; 2005b, hereafter BK05b). These latest very sensitive H I absorption observations were undertaken with the Westerbork radio telescope in the directions of four continuum sources, all located at high Galactic latitude ($b \sim 80^\circ$) and relatively close to each other. The peak H I emission in these directions is very low, 2–5 K only. For three out of four sources multiple absorption lines were detected, with a peak optical depth of only 0.1%–2%.

BK05b discovered cold H I clouds with the lowest H I column densities ever detected for cold interstellar clouds, more than 30 times lower than what is expected for the smallest CNM clouds. Fascinated by the discoveries of BK05b, and desiring to

confirm their reality, we repeated their observations for two sources, 3C 286 and 3C 287, with the Arecibo telescope. We easily confirmed findings by BK05b for 3C 286. Against 3C 287 we see only a weak feature with too little signal-to-noise ratio (S/N) to include in our discussion.

In this paper we report on the Arecibo observations of 3C 286 and 3C 287 and discuss implications of these findings. Our main aim is to emphasize the existence of cold CNM clouds with H I column densities $\sim 10^{18} \text{ cm}^{-2}$, to discuss these data in the context of previous observational results, and to initiate discussion on the possible origin of these clouds, as well as their importance in the ISM. In § 2 we briefly outline our observing and data processing methods. Section 3 presents basic properties of cold H I clouds in the directions of 3C 286 and 3C 287. A comparison of these clouds with CNM components found in previous observational studies is given in § 4. In § 5 we discuss several different possibilities for the formation of these clouds.

2. OBSERVATIONS AND DATA PROCESSING

The observations were conducted with the Arecibo telescope.¹ Several hours of observing time were granted at the discretion of the Arecibo Observatory director Sixto Gonzalez to evaluate the viability of future very sensitive H I absorption measurements. The observing procedure was the same as in Heiles & Troland (2003a). A specific observing pattern, developed in Heiles & Troland (2003a), was performed to estimate the “expected” H I emission profile. This pattern generates one on-source spectrum and 16 off-source spectra, which are used to derive first and second derivatives of the H I emission on the sky.

The final velocity resolution is 0.16 km s^{-1} . The final rms noise level in the absorption spectra is 5×10^{-4} over 0.5 km s^{-1} channels (or 3×10^{-4} over 1 km s^{-1} channels). After the data reduction, for both sources 3C 286 and 3C 287 we have an H I absorption ($e^{-\tau(v)}$) and an H I emission spectrum [$T_B(v)$; note that this is the emission spectrum that would be observed in the absence of the continuum source].

We next employed the technique by Heiles & Troland (2003a) to estimate the spin temperature for the CNM clouds. This technique assumes that the CNM contributes to both H I absorption

¹ The Arecibo Observatory is part of the National Astronomy and Ionosphere Center, operated by Cornell University under a cooperative agreement with the National Science Foundation.

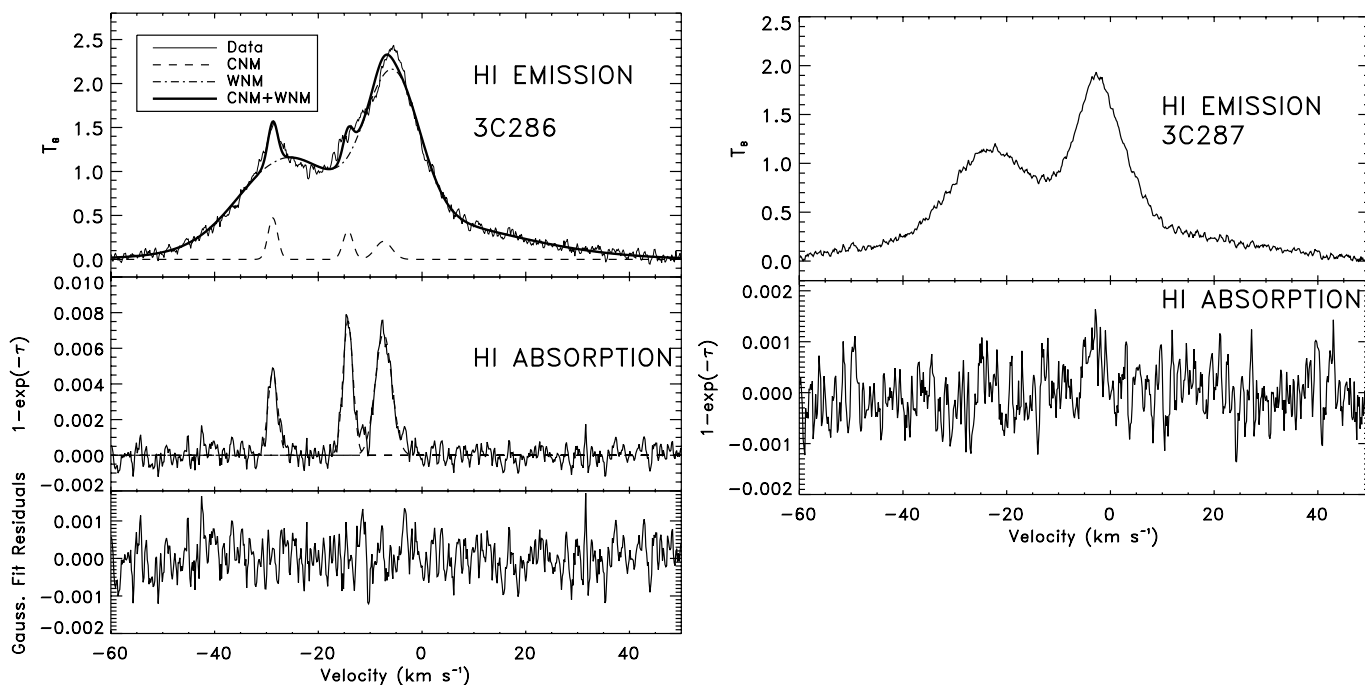


FIG. 1.—H I emission and absorption spectra for 3C 286 (*left*) and 3C 287 (*right*) obtained with the Arecibo telescope. For 3C 286, three CNM components were detected. For both sources the top panel shows the H I emission profile. In the case of 3C 286, separate contributions from the CNM and WNM to the H I emission profile are shown with dashed and dot-dashed lines, respectively, while the final, simultaneous fit is shown with the thick solid line. The middle panels shows the H I absorption spectra. For 3C 286, three separate Gaussian functions were fitted (*dashed line*). Note that $1 - \exp(-\tau) \approx \tau$, as the H I optical depths are very small. The bottom panel for 3C 286 shows the residuals of the absorption profile after the fitting procedure. Note that original spectra have been boxcar smoothed by three channels; the resulting rms noise in the resulting absorption spectra is 5×10^{-4} .

and emission spectra, while the warm neutral medium (WNM) contributes only to the H I emission spectrum. The technique is based on the Gaussian decomposition of both absorption and emission spectra, and it takes into account the fact that a certain fraction of the WNM gas may be located in front of the CNM clouds, resulting in only a portion of the WNM being absorbed by the CNM. We note, however, that this technique may not be applicable for the case when the CNM occupies a solid angle significantly smaller than that of the Arecibo telescope beam ($\text{FWHM} = 3'.5$), as is most likely the case with some CNM components we find in § 4.3. In this case, the observed absorption spectrum may not correspond to the absorption that would be seen from all gas included in the emission spectrum, and hence a direct comparison of the H I absorption and emission spectra may not be a valid approach. For those very small clouds that do not fill the beam, our emission intensity is underestimated, resulting in the derived spin temperature being too low. Thus, we should regard our derived spin temperatures as lower limits. Another issue regarding this technique is the use of Gaussian functions to represent the CNM absorption profiles. Heiles & Troland (2003a) discussed pros and cons of this approach in some detail.

3. RESULTS

In Figure 1 we show H I emission and absorption spectra for 3C 286 (*left*) and 3C 287 (*right*). Three panels are shown for 3C 286. In the top panel the H I emission spectrum (a main beam efficiency of 0.9 was used to convert this spectrum from the antenna temperature units to the brightness temperature scale) and separate contributions from the CNM and WNM to the H I brightness temperature are shown with different lines; the final (simultaneous) fit to the spectrum is also overlaid. In the middle panel the H I absorption spectrum with fitted individual Gaussian

components is shown. We detect three CNM components toward 3C 286. In the bottom panel the residuals of the absorption spectrum for 3C 286 after the fitting process are shown. These random-looking residuals demonstrate that the fit is perfect at the present level of S/N and that the Gaussian representation of CNM components is valid in this case. In the case of 3C 287 we have only a marginal detection at this stage.

3.1. 3C 286

The H I absorption spectrum shows three distinct features, in good agreement with BK05b. We have fitted them with three Gaussian functions centered at LSR velocities -28.8 , -14.3 , and -7.4 km s^{-1} (Table 1). The spin temperature is well constrained at the 10% level for the first two Gaussian components. The contribution to the H I emission profile from the last CNM component appears to be very small, resulting in its spin temperature not being well constrained (60% level). The resulting H I column densities are directly proportional to these temperatures and are given in Table 1 (col. [8]). They are all very low, $< 1.5 \times 10^{18} \text{ cm}^{-2}$. Table 1 also provides upper limits to $N(\text{H I})$ assuming that the line widths are thermal, in which case the spin temperatures are equal to $T_{k,\text{max}}$. Even these are small for the first two components, a few times 10^{18} cm^{-2} .

We compare our results with those of BK05b, who also found three distinct absorption features at velocities and with peak optical depths very similar to ours. They fitted simultaneously H I emission and absorption spectra as resulting from spherically symmetric, isobaric clouds with an exponential H I volume density distribution. Assuming a representative spin temperature of 100 K, their estimated H I column density for absorption features is $(0.4\text{--}8) \times 10^{18} \text{ cm}^{-2}$ (BK05b).

Using our derived temperatures from Table 1, the three absorption components sum to the total estimated CNM column

TABLE 1
PROPERTIES OF CNM CLOUDS IN THE DIRECTIONS OF 3C 286 AND 3C 287

Source (1)	l/b (deg/deg) (2)	τ_{\max} (3)	V_{LSR}^a (km s $^{-1}$) (4)	FWHM a (km s $^{-1}$) (5)	T_{spin} (K) (6)	$T_{k,\max}$ (K) (7)	$N(\text{H I})_{\text{CNM}}$ (10^{20} cm $^{-2}$) (8)	$N(\text{H I})_{\text{CNM}}^{\text{upper}}$ (10^{20} cm $^{-2}$) (9)
3C 286	56.5/80.7	0.0047 ± 0.0003	-28.8	2.2	89 ± 7	106	0.018 ± 0.002	0.021
		0.0076 ± 0.0003	-14.3	2.3	37 ± 4	115	0.013 ± 0.002	0.039
		0.0069 ± 0.0002	-7.4	3.8	30 ± 20	315	0.015 ± 0.008	0.161
3C 287	22.5/81.0	<0.002	~ -3.2	3	100	200	<0.012	<0.023

NOTE.—The upper limit on H I column density, $N(\text{H I})_{\text{CNM}}^{\text{upper}}$, was derived using $T_{k,\max}$ instead of T_{spin} .

^a The uncertainty in the central velocity and FWHM is 0.1 km s $^{-1}$ for 3C 286.

density 3.9×10^{18} cm $^{-2}$, while the total WNM column density is 1.1×10^{20} cm $^{-2}$. This means that the CNM comprises only 4% of the total H I column density in this direction.

3.2. 3C 287

Neither Dickey et al. (1978) nor BK05b detected absorption features in this direction, indicating that the peak optical depth must be <0.01 . We have only a marginal detection, at a 3σ level, of an absorption feature at the LSR velocity of -3.2 km s $^{-1}$ with a peak optical depth of only 10^{-3} . As the S/N for this feature is too low, we place only an upper limit for the CNM in this direction. Future observations will be able to clarify this detection. Our upper limit on the peak optical depth (at a 5σ level) is ~ 0.002 . If we assume a hypothetical CNM component with $\tau_{\max} < 0.002$, $T_{\text{spin}} = 100$ K, and $\text{FWHM} = 3$ km s $^{-1}$, then $N(\text{H I})_{\text{CNM}} < 1.2 \times 10^{18}$ cm $^{-2}$. As the total WNM column density in this direction is 1.1×10^{20} cm $^{-2}$, the CNM would comprise less than 2% of the total H I column density toward 3C 287.

4. DISCUSSION: OBSERVATIONAL ISSUES

4.1. A New Population of Interstellar Clouds?

The detected peak optical depths here and in BK05b are among the lowest ever detected for Galactic CNM clouds. They appear to represent a new population of CNM clouds that is not represented by the existing observational data and summaries.

For 3C 286 and 3C 287, the estimated H I column densities are all $<1.6 \times 10^{18}$ cm $^{-2}$, more than 30 times lower than what is traditionally expected for the smallest CNM clouds (McKee & Ostriker 1977). Clearly, the CNM clouds in the directions of 3C 286 and 3C 287 have a very low H I column density, and as shown in § 3, these CNM clouds comprise only $<2\%$ – 4% of the total measured H I column density.

But how unusual are these low CNM columns? In the most recent H I absorption survey with the Arecibo telescope, Heiles & Troland (2003b) found that the median H I column density for CNM clouds is 5×10^{19} cm $^{-2}$ [note that the sensitivity of this survey is $\Delta N(\text{H I}) \sim 10^{18}$ cm $^{-2}$]. HT05 provided statistical distributions of the fundamental parameters: H I column density, temperature, turbulence, and magnetic field. They found that the observed probability density function (PDF) of $N(\text{H I})$, for sources primarily at high Galactic latitudes, is well approximated by N^{-1} between the limits given by

$$N_{\perp 20, \min} = 0.026_{-0.010}^{+0.019} \quad (1a)$$

$$N_{\perp 20, \max} = 2.6_{-1.2}^{+1.9}, \quad (1b)$$

where the subscript 20 means units of 10^{20} cm $^{-2}$.

HT05 regarded the lower limit ($N_{\perp 20, \min}$) to be real, not an observational result imposed by the lack of sensitivity. However,

the presence of three weak absorption components toward 3C 286—one of HT05's sight lines—shows that their sensitivity estimate was optimistic. HT05's PDF of equations (1a) and (1b) certainly applies to their sources with strong absorption lines, which have received a large amount of integration time for measuring Zeeman splitting. But it appears that there is a new population of CNM components that is unrepresented in their survey.

4.2. The CNM Fraction

McKee & Ostriker (1977) predicted the CNM to form $\sim 95\%$ of the total H I. Observers have traditionally found smaller column density fractions; for example, Heiles & Troland (2003b) found that the majority of sight lines have a CNM column density fraction $<30\%$, while the WNM fraction is $\sim 61\%$. This WNM column density fraction translates to a volume fraction of ~ 0.5 . Wolfire et al. (2003) have updated the theory of ISM neutral phases and slightly refined the values for the WNM pressure and density; these refinements bring the observed WNM volume fraction to 0.8. However, sight lines toward 3C 286 and 3C 287 have much smaller fractions of the CNM column density, $\sim 4\%$ and $\lesssim 2\%$, respectively. These echo the small fractions found by HT05, who found 19 (out of 79) lines of sight with no detectable CNM; 3C 286 was one of these, so perhaps we should take their nondetections to indicate a possible representative upper limit of a few percent for this CNM/total H I ratio.

These small CNM fractions might be a problem for the theory. Alternatively, the particular sight lines having small CNM fractions might lie in special regions affected by energetic processes that have temporarily destroyed the CNM. In fact, sight lines toward 3C 286 and 3C 287 pass through the north Galactic pole region, where Kulkarni & Fich (1985) already noticed that about 50% of H I is infalling toward the plane, while warm H I occupies about 40%. This question needs further investigation.

4.3. Are Low Column Density Clouds Related to the Tiny-Scale Atomic Structure?

A second population of low-column CNM clouds are those often referred to as the tiny-scale atomic structure (TSAS). The TSAS size scale is inferred from time variability of H I absorption profiles against pulsars or very long baseline interferometry (VLBI) imaging of extragalactic continuum sources and ranges from a few AU to a few hundreds of AU. TSAS typically has $N(\text{H I})$ somewhat higher than our Table 1 components, namely, from $\sim 3 \times 10^{18}$ to $\sim 2 \times 10^{19}$ cm $^{-2}$ (Heiles 1997). Recently, S. Stanimirović et al. (2005, in preparation) found persistent variations in the H I optical depth profiles of PSR B1929+10 that indicate structure in the cold H I with $N(\text{H I}) \sim 2 \times 10^{18}$ cm $^{-2}$. With these column densities and small sizes, the TSAS must be overpressured with respect to most of the ISM. Thus, TSAS

features are thought to be very dense and overpressured, with $n(\text{H I})$ and P reaching values up to $\sim 10^4 \text{ cm}^{-3}$ and $\sim 10^6 \text{ K cm}^{-3}$, respectively.

If we assume that our low column density CNM clouds toward 3C 286 and 3C 287 are similarly overpressured, then the implied size scale is even smaller than the typical TSAS scale, because our column densities are somewhat smaller. Alternatively, if our CNM components are at the standard ISM pressure, with $nT \sim 3000 \text{ cm}^{-3} \text{ K}$ (Jenkins & Tripp 2001), then their H I volume densities are $n \sim 20\text{--}100 \text{ cm}^{-3}$ and the implied size scales are $N(\text{H I})/n(\text{H I}) \sim 800\text{--}4000 \text{ AU}$. Even these larger sizes are not too much higher than the inferred sizes for much of the TSAS.

Another indication that the low column density clouds could be related to TSAS comes from direct interferometric imaging. Over a range of velocities, BK05b found compact emission clumps with a FWHM of $1\text{--}2 \text{ km s}^{-1}$ and an intrinsic size of $30''$; at an assumed distance of 100 pc, this corresponds to a plane-on-the-sky size of about 3000 AU. This morphology is distinctly different from the clumpy sheetlike model of the CNM suggested by Heiles & Troland (2003b) and may point again to a distinctly different origin of these clouds. The compact clumps at apparently random locations may be suggestive of fluctuations in the distribution of H I optical depth over a wide range of spatial scales, rather than the presence of distinct physical entities. If the low column density H I clouds and TSAS features have a common origin, then TSAS is significantly more abundant in the ISM, and with significantly lower optical depths, than what is expected theoretically if the TSAS is simply the low size scale extension of the interstellar turbulence spectrum, as discussed by Deshpande (2000).

Perhaps the TSAS is characterized by a range of column densities and pressures, with the classical absorption observations presented here sampling the low-density end and the pulsar/VLBI observations, which are less sensitive, the (possibly much rarer) high-density end.

5. DISCUSSION: THEORETICAL CONSIDERATIONS

We discuss some current theoretical approaches that can lead to the production of cold clouds in the ISM with column densities similar to what is found observationally. These comprise two general classes: clouds that are long-lived and can be characterized as semipermanent structures, and transient clouds.

5.1. Semipermanent Clouds

5.1.1. Evaporation Versus Condensation

In the well-accepted theory of McKee & Ostriker (1977), the CNM resides within warmer phases. However, it is expected that different phases are separated by an interface region through which heat flows between the two phases. The interface is a surface of transition, where, for small CNM clouds, the CNM evaporates into the warmer medium and, for large CNM clouds, the warmer medium condenses onto the CNM. The classical evaporation theory (McKee & Cowie 1977) predicts a critical radius for CNM clouds at which radiative losses balance the conductive heat input and at which the cloud neither evaporates nor condenses. Clouds smaller than the critical radius evaporate, while clouds larger than the critical radius accrete by condensation of the surroundings. McKee & Cowie (1977) estimated the characteristic scale length for different temperature layers in the interface region. From there, in the case of the least intrusive interface, CNM to WNM with an intercloud temperature of $10^2\text{--}10^4 \text{ K}$, the expected lower limit on the column density of the interface region is about $N(\text{H I}) \sim 3 \times 10^{17} \text{ cm}^{-2}$. Higher inter-

cloud temperatures are more intrusive; for example, for $T \sim 10^6 \text{ K}$ the interface region would have several temperature layers with different column densities, adding up to a total column density $> 2 \times 10^{18} \text{ cm}^{-2}$ (mainly ionized, however).

In the case of the least intrusive interface with the WNM, the cloud critical radius (R_{rad}) times the density of the intercloud region (we assume $n_{\text{WNM}} = 0.5 \text{ cm}^{-3}$) is about $5 \times 10^{16} \text{ cm}^{-2}$ (from Fig. 2 in McKee & Cowie 1977). The expected critical radius is then $R_{\text{rad}} \sim 6 \times 10^3 \text{ AU}$, meaning that clouds smaller than this size evaporate, while CNM clouds larger than R_{rad} accrete the WNM by condensation. These small, evaporating clouds are surprisingly long-lived; the typical evaporation timescale is of the order of 10^6 yr (we have assumed a mass-loss rate of $1.2 \times 10^{23} \text{ g yr}^{-1}$ and $n_{\text{CNM}} = 30 \text{ cm}^{-3}$, and used eq. [47] in McKee & Cowie 1977).

The estimated sizes for the low $N(\text{H I})$ clouds in § 4.3 are all below the critical cloud radius even in the case of the least intrusive WNM. These CNM clouds, protected from ionization by large WNM envelopes, should be evaporating, but over long timescales, and hence could be common in the ISM.

5.1.2. Condensation of WNM into CNM Induced by Turbulence?

Recent numerical simulations by Audit & Hennebelle (2005) show that a collision of incoming turbulent flows can initiate condensation of WNM into cold neutral clouds. This model hence naturally explains the formation of cold clouds at high Galactic latitudes. In the simulations, a collision of incoming WNM streams creates a thermally unstable region of higher density and pressure but lower temperature, which further fragments into cold structures. The thermally unstable gas has a filamentary morphology, and its fragmentation into cold clouds is promoted and controlled by turbulence. Typical properties of cold clouds formed in the simulations are $n \sim 50 \text{ cm}^{-3}$, $T \sim 80 \text{ K}$, and $R \sim 0.1 \text{ pc}$. In addition, many small clouds, with sizes reaching the numerical resolution of 0.02 pc , were found.

These cold clouds are thermally stable and long-lived; in the case of stronger turbulence they are more roundish, while a weaker turbulence is responsible for more elongated morphology of cold clouds. The simulations show that the fraction of cold gas ranges from 10% in a strong turbulent case to about 30% in a weak turbulent case. These fractions are larger than our observed fractions; perhaps further refinement of the models can produce better agreement. In fact, it is known that the CNM fraction and the CNM column density depend also on the input mean thermal pressure and the input velocity of colliding flows, which are free parameters in the simulations and could be better constrained from H I observations (P. Hennebelle 2005, private communication).

These simulations show that a collision of turbulent WNM streams is capable of producing a large number of small CNM clouds with low column densities and not confined to the Galactic plane. The CNM clouds are thermally stable and embedded in large, unstable WNM filaments. The abundance of cold clouds, as well as their properties, depends heavily on the properties of the underlying turbulent flows. In a similar approach, Koyama & Inutsuka (2002) showed that a thermally unstable shock-compressed layer can also fragment into small, cold, turbulent condensations.

5.2. Transient Clouds

A CNM cloud is normally pictured as an entity in quasi-equilibrium with its surroundings. A contrasting viewpoint, stimulated by the recent flurry of numerical simulations of interstellar turbulence, envisions the clouds as dynamic entities that are

constantly changing in response to the turbulent “weather” (for a review, see Mac Low & Klessen 2004). For example, Vazquez-Semadeni et al. (1997) performed simulations that produced many clouds with very small sizes and low column densities ($<10^{19} \text{ cm}^{-2}$). These clouds are out of equilibrium and probably very transient.

In MHD simulations by Vazquez-Semadeni et al. (1997), cold clouds form at the interfaces of expanding shells. Their typical size is $\sim 1\text{--}200$ pc (see Fig. 5 in Vazquez-Semadeni et al. 1997), and for any given size the mean volume density of clouds ranges from ~ 2 to 60 cm^{-3} . Clouds are found to have irregular and filamentary shapes. The cloud column density ranges from 10^{19} to 10^{20} cm^{-2} , while a typical FWHM is from 2 to 15 km s^{-1} .

Qualitatively different is the interaction of shocks with pre-existing clouds, as opposed to clouds forming within shocks. F. Nakamura, R. I. Klein, C. F. McKee & R. Fisher (2005, private communication) find that when a supernova shock hits a pre-existing cloud, the cloud is torn up into small pieces (“shreds”) with a velocity dispersion of several km s^{-1} . Some of the predicted properties of these shreds appear close to what we observe. Further advances in this area are eagerly awaited for more detailed comparison with observations.

In summary, several properties predicted by numerical simulations do not match our observations very well, but others do. These theoretical efforts are in their early stages and are developing rapidly. We can expect rapid evolution in the future.

6. SUMMARY AND CONCLUSIONS

Recently, BK05b discovered several cold H I clouds at high Galactic latitudes with small H I optical depths. We have confirmed their detections in the direction of 3C 286 and added an additional weak upper limit to this set. We have found the absorption components to be well represented by Gaussian functions and have derived their spin temperatures and H I column densities. These clouds have H I column densities among the lowest ever detected for the CNM features and could represent a new population of interstellar clouds. We have compared them with the TSAS detected by time-variable pulsar absorption lines and VLBI and concluded that they might be of the same general class. These observational techniques used for detecting TSAS might highlight the high volume density and pressure members of this class, while the more traditional emission/absorption observations highlight the lower volume density/pressure members.

The sight lines toward 3C 286 and 3C 287 have very low CNM fractions. Similarly low fractions have been found for 24% of continuum sources in the large H I absorption line survey by Heiles & Troland (2003a). Such low CNM fractions are not theoretically predicted. This either might be a problem with the theories or might indicate that some sight lines are special, traversing regions from which CNM has been removed perhaps by energetic processes.

We have investigated briefly three different theoretical approaches for the production of cold, low column density clouds in the ISM. Two of these envision the CNM clouds as semipermanent entities. The third envisions the clouds as transitory structures. CNM clouds may be formed by cooling and condensation in colliding turbulent streams of WNM, whereby cold clouds are stable discrete entities surrounded by thermally unstable WNM filaments. Alternatively, many numerical simulations envision cold clouds being transient and constantly changing phenomena in the turbulent ISM. Theory and observations are not in full accord regarding the fraction of CNM gas and its column densities. Further work in both observations and theory is called for.

Observationally, it is essential to quantify how common these clouds are in the ISM and whether they are related to some local events, such as stellar winds or large-scale atomic flows. We need to increase the statistical sample to establish the probability density function of the column density in the vicinity of its current lower cutoff, where most of the low $N(\text{H I})$ clouds are found. In addition, we need to more firmly determine the relationship between the CNM components found here and TSAS.

We are grateful to telescope operators at the Arecibo Observatory for their help in conducting these observations, particularly to William Torres and Norberto Despiau. We would also like to thank Hector Hernandez and Sixto Gonzalez for prompt scheduling of this project. It is a pleasure to acknowledge stimulating discussions with Patrick Hennebelle, Miller Goss, Joel Weisberg, Nissim Kanekar, Robert Braun, and Chris McKee. S. S. is indebted to Chris McKee for pointing out an error in an earlier version of this manuscript. We also thank an anonymous referee for valuable suggestions. Support by NSF grants AST 00-97417 and AST 99-81308 is gratefully acknowledged.

REFERENCES

- Audit, E., & Hennebelle, P. 2005, *A&A*, 433, 1
 Braun, R., & Kanekar, N. 2005a, in *The Initial Mass Function 50 Years Later*, ed. E. Corbelli, F. Palla, & H. Zinnecker (Dordrecht: Springer), in press (astro-ph/0409427)
 ———. 2005b, *A&A*, 436, L53 (BK05b)
 Deshpande, A. A. 2000, *MNRAS*, 317, 199
 Dickey, J. M., Terzian, Y., & Salpeter, E. E. 1978, *ApJS*, 36, 77
 Field, G. B., Goldsmith, D. W., & Habing, H. J. 1969, *ApJ*, 155, L149
 Heiles, C. 1997, *ApJ*, 481, 193
 Heiles, C., & Troland, T. H. 2003a, *ApJS*, 145, 329
 ———. 2003b, *ApJ*, 586, 1067
 Heiles, C., & Troland, T. H. 2005, *ApJ*, 624, 773 (HT05)
 Jenkins, E. B., & Tripp, T. M. 2001, *ApJS*, 137, 297
 Koyama, H., & Inutsuka, S. 2002, *ApJ*, 564, L97
 Kulkarni, S. R., & Fich, M. 1985, *ApJ*, 289, 792
 Mac Low, M., & Klessen, R. S. 2004, *Rev. Mod. Phys.*, 76, 125
 McKee, C. F., & Cowie, L. L. 1977, *ApJ*, 215, 213
 McKee, C. F., & Ostriker, J. P. 1977, *ApJ*, 218, 148
 Vazquez-Semadeni, E., Ballesteros-Paredes, J., & Rodriguez, L. F. 1997, *ApJ*, 474, 292
 Wolfire, M. G., McKee, C. F., Hollenbach, D., & Tielens, A. G. G. M. 2003, *ApJ*, 587, 278